Graphene phytotoxicity in the seedling stage of cabbage, tomato, red spinach, and lettuce

Parvin Begum, Refi Ikhtiari and Bunshi Fugetsu*

Laboratory of Environmental Medical Chemistry, Graduate School of Environmental Science, Hokkaido University, Sapporo 060-0810, Japan

* *Corresponding author*: Fax: 81 11 7062272

E-mail address: hu@ees.hokudai.ac.jp (B. Fugetsu).

ABSTRACT

The effects of graphene on root and shoot growth, biomass, shape, cell death, and reactive oxygen species (ROS) of cabbage, tomato, red spinach, and lettuce, were investigated using a concentration range from 500 to 2000 mg/L. The results of the combined morphological and physiological analyses indicate that after 20 days of exposure under our experimental conditions, graphene significantly inhibited plant growth and biomass compared to a control. The number and size of leaves of the graphene-treated plants were reduced in a dose-dependent manner. Significant effects also were detected showing a concentration-dependent increase in ROS and cell death as well as visible symptoms of necrotic lesions, indicating graphene-induced adverse effects on cabbage, tomato, and red spinach mediated by oxidative stress necrosis. Little or no significant toxic effect was observed with lettuce seedlings under the same conditions. The potential effect of graphene largely depends on dose, exposure time, and plant species and deserves further attention.

1. Introduction

The use of nanostructures with unusual novel properties in agriculture [1] and for technological applications has been an active and exciting area of research in recent years. Graphene, the most recently discovered carbon allotrope, is a two-dimensional building block of atomic thickness that can be stacked into three-dimensional graphite, rolled into one-dimensional nanotubes, or wrapped into zero-dimensional fullerenes [2]. The unique electronic and transport properties of graphene [3], compatible with existing manufacturing processes [4], and the absence of the energy gap in the electronic spectra have opened up increasingly rich possibilities in the development of future electronic devices [3,5] and the graphene-based quantum electronics [6] that offer many benefits. If these trends in nanotechnology continue, graphene may ultimately be released into the aquatic, terrestrial, and atmospheric environments, where its fate and behavior are largely unknown. Exposure to nanoparticles in higher plants is expected to have an effect because these plants strongly interact with their atmospheric environments [7]. The nanoparticles, with their ultra-small size, specific shape, geometric structure, and unique properties, may have the potential for increased toxicity [8-11]. Nanoparticles can drastically modify their physicochemical properties compared to particles of bulk size [12]. Carbon nanoparticles can penetrate plant cells [13,14] and induce phytotoxicity at high doses [15-17], leading some authors to conclude that certain carbon nanoparticles are not 100% safe. Therefore, great caution is suggested when considering the introduction of nanoparticle-based products to the market, and there is an urgent need for research related to the broad area of nanotoxicology. A recent study, for example, has

pointed to the possible adverse effects of graphene on human health [18] and in bacteria [19].

In response to these concerns, we explored whether graphene can induce phytotoxicity at high doses in terrestrial plants grown hydroponically and exposed to varying concentrations (0 to 2000 mg/L) of graphene. According to the US EPA guidelines [20] the highest concentration of graphene used for this study was 2000 mg/L. In addition, Rico *et al.* [21] have described that nanoparticles showing a manifest toxic effect on the food crops commonly appears in the range of concentration of 1000−4000 mg/L of the nanoparticles. Toxicity studies on the food crops were commonly carried out at high concentrations (2000~5000 mg/L) of the nanoparticles [17, 22, 23]. Khodakovskaya *et al*. [13] reported insignificant toxicities of graphene in the growth of tomato, although they used only one low concentration (50 μg⁄mL) of chemically functionalized graphene with few layers and with a thickness of 2–5 nm. In a study by Says *et al*. [24], carbon nanoparticle functionalization led to a remarkable decline in toxic effects. The effects of nanoparticles on different plant species can vary greatly with plant growth stages and method and duration of exposure and depend also on nanoparticle size, concentration, chemical composition, surface structure, solubility, shape, and aggregation [12].

Thus, to our knowledge, the possible adverse effect of graphene in terrestrial plants is almost totally unknown. Here, we use cabbage, tomato, red spinach, and lettuce as the selected crops to investigate the toxic effects of graphene and to identify appropriate target plant species for further studies associated with graphene. Potential targets include various terrestrial plants that are normally protected by specific barriers such as a cell

wall. Targeting can be made more effective by prolonged exposure of different plant species to carbon nanoparticles and application of a high concentration, which can lead to aggregation on the root surface [25], penetration within the cells [13], and a contribution to toxic effects [15,16,26]. This report is the first to describe the phytotoxic effect of graphene in terms of seedling growth, cell death, reactive oxygen species (ROS) generation, and morphology change. Our results showed the greatest toxic effect of graphene on cabbage and tomato, followed by red spinach, with no clear toxic effect for lettuce.

2. Experimental

2.1. *Chemicals and seeds*

Chemicals used in this experiment were purchased from Kanto Chemical Co. Inc., Wako Pure Chemical Industries, Ltd., or Sigma Aldrich Inc., Japan. Seeds of three plant species (cabbage, *Brassica oleracea* var. capitata; tomato, *Lycopersicon esculentum*; and lettuce, *Lactuca sativa*) used in this study were purchased from Homac, Sapporo, Japan. Red spinach (*Amaranthus tricolor* L. and also *Amaranthus lividus* L.) seeds were purchased from Dhaka, Bangladesh.

2.2. *Preparation of water-soluble graphene*

Water-soluble graphene was obtained from natural graphite (SP-1, Bay Carbon) by using a modified Hummers and Offeman's method [27]. In a typical treatment, 100 g of the graphite powders and 50 g of sodium nitrate and 2000 mL sulfuric acid were mixed in an ice bath. Next, 100 g of potassium permanganate was slowly added and well mixed. Once

mixed, the suspension was placed in a water bath at 35 ± 3 ºC and mixed for about 30 min. About 5 L of deionized water was added to the suspension, the temperature was increased to 90 ± 3 ºC, and the suspension was mixed further for about 30 min. The suspension was finally diluted to about 10 L with warm deionized water and about 200 mL of 30 wt% hydrogen peroxide (H_2O_2). The warm suspension was filtered, and a yellow-brown filtered cake was obtained. The filtered cake was carefully washed with a large amount of warm deionized water and then dispersed in deionized water by mechanical mixing to prepare a stock graphene aqueous suspension containing approximately 2 wt% water-soluble graphene. An aqueous 0.1 mol/l sodium hydroxide solution was used to neutralize the graphene solution to a pH 6.32.

2.3. *Seedling exposure*

The sterile seeds of the selected plant species were soaked in solution with different concentrations (0, 500, 1000, and 2000 mg/L) of graphene overnight at 25 °C in the dark. Seeds were placed on wet filter paper and then exposed to 3 mL of the test solution with and without graphene and incubated at 25 °C until germination. After germination, the number of germinated seeds was counted. The seedlings were transferred to plastic pots containing 200 mL Modified Hoagland Medium [28]. Values of pH of the Hoagland medium remained almost unchanged during the 20 days of the graphene exposure. They were restricted in 6.3–6.5. These pH values were desirable for plant growth [29]. Seedlings were treated with different concentrations of graphene solution (0, 500, 1000, or 2000 mg/L). At 2000 mg/L graphene was stable with very little settling.

2.4. *Root, shoot growth, and leaf characters*

After 20 days of exposure, roots and shoots were separated and washed with water to remove the growth medium and dried with wipes to remove the surface water. Their length and fresh weights were recorded. Leaf numbers were counted and leaf area measured using a RHIZO 2004b instrument.

2.5. *ROS measurements and H_2O_2 detection*

For visualization and measurement of ROS by spectroscopy, oxidatively sensitive probes 2',7'-dichlorofluorescein diacetate (DCFH-DA) and 3,3'-diaminobenzidine (DAB) were used. Fresh leaves of the treated and untreated plants were incubated in DCFH-DA for 2h for the ROS measurements and the H_2O_2 detection. After three PBS (phosphate-buffered saline) rinses, the images for visualization were captured using fluorescence microscopy (Olympus IX70). We performed a measurement of DCFH fluorescence intensity in the leaves using a spectrofluorometer (Hitachi F-4500) by suspending the leaves in PBS buffer with an excitation wavelength at 485 nm and emission wavelength at 522 nm. The values were expressed as % of fluorescence intensity relative to control. This experiment was performed without exposure to light.

H_2O_2 was detected using DAB by the method previously described by Thordal-Christensen *et al*. [30]. The fresh leaves from 20-day-old treated and untreated plants were placed in 1 mg/mL DAB-HCl, pH 3.2–3.8 and incubated under vacuum for ~8 h. DAB deposits were revealed after washing leaves in boiled 100% (v/v) ethanol for 15 min to decolorize the leaves except for the deep brown polymerization product from the reaction of DAB with H_2O_2. The images were observed and recorded using light

microscopy (Transmit Light Microscope BX51, With Olympus DP72 Camera). The amount of formazan formation in leaves was measured spectrophotometrically at A_{700} (V-530 UV/UISNIR Spectrophotometer, Jasco, Japan) after leaves were ground in liquid nitrogen and solubilized in a mixture of 2 M KOH and DMSO at a ratio of 1:1.167 (v/v).

2.6. *Evaluation of cell death*

The cell death of the selected plant roots was evaluated by the method previously described by Baker and Mock [31] using Evans blue (0.025% v/v) for 2 h after 20 days of exposure to different concentrations (0, 500, 1000, and 2000 mg/L) of graphene. For quantitative assessment, after several washes with water, the Evans blue was extracted using 1% (w/v) SDS in 50% (v/v) methanol at 50 °C for 15 min, and the absorbance (optical density) was measured spectrophotometrically at 597 nm (V-530 UV/UISNIR Spectrophotometer, Jasco, Japan). Cell death was expressed as absorbance of treated roots in relation to untreated roots (control).

Cell death was also evaluated by measurement of ion leakage from leaf. The percent of injury of the membrane was measured from the electrolyte leakage of treated and untreated plants by a conductivity method based on the procedure of Lutts *et al*. [32] with some modifications. Leaf samples (100 mg) were placed in test tubes containing 10 mL of distilled water after three washes with distilled water to remove surface contamination. Test tubes were covered and incubated at room temperature (25 °C) on a shaker (100 rpm) for 24 h. Electrical conductivity of the solution (L_t) was determined. Samples were then autoclaved at 120 °C for 20 min, and a final conductivity reading (L_0) was obtained upon equilibration at 25 °C. Electrolyte leakage was defined as: Electrolyte leakage (%)

= $(L_t/L_0) \times 100$. The extent of membrane injury (leakage of electrolytes) from cells was determined with a portable conductivity meter (pH/Cond Meter, Horiba D-54).

2.7. *Morphological observation by atomic force microscopy (AFM), scanning electron microscopy (SEM) and transmission electron microscopy (TEM)*

For AFM, an Agilent Series 5500 AFM instrument was used. The samples were prepared by casting a diluted aqueous graphene suspension on the surfaces of mica. The images were obtained using the tapping mode at a scanning rate of 1 Hz. For SEM, a few drops of the graphene suspension were deposited on the aluminum stub, dried, sputter-coated, and observed using a Hitachi S-4000 SEM (Hitachi, Ibaraki, Japan) with an acceleration voltage of 10 kV. For SEM, the roots were fixed in 2.5% glutaraldehyde (GA) and 2% paraformaldehyde (PA) in 0.1 M phosphate buffer (PB), pH 7.4, postfixed in 1% osmium tetroxide, dehydrated, critical-point dried, sputter-coated, and observed. For TEM, the graphene were homogeneously dispersed in 2-propanol under ultrasonication for 30 min. A few drops of the suspension were deposited on the TEM grid covered with a Formvar membrane, dried, and evacuated before analysis. For root TEM, the roots were fixed in 2.5% GA and 2% PA in 0.1 M PB buffer, pH 7.4, postfixed in 1% osmium tetroxide, dehydrated, infiltrated with ethanol:Epon, embedded in pure Epon and polymerized at 60°C for 2 days. Ultra-thin sections were stained with 2% uranyl acetate and lead citrate. The preparations were observed using a Hitachi H-800 TEM. The acceleration voltage was 75 kV.

Statistical analysis

Each treatment was conducted in triplicate. Phytotoxicity endpoints for all measurements were compared to those of the unexposed controls. Statistical analysis was performed

using the Student's t-test; values of $P \leq 0.01$ were considered significant. Data are presented as mean ± SD (standard deviation).

3. Results and discussion

A previous study uncovered evidence supporting that carbon-based nanoparticles have adverse effects on terrestrial plants [17], opening the way to further investigation. Consequently, we assessed the potential impact of graphene on the growth of tomato, cabbage, red spinach, and lettuce based on tests suggested and encoded by USEPA guidelines [20], which include consideration of studies on seed germination and seedling growth (root and shoot growth, leaf number), often accompanied by other evaluations of cell death, ROS production, and morphological studies using SEM, useful for obtaining evidence of *in situ* symptoms of possible toxicity. Altogether, the current work investigating the potential effect of graphene demonstrates possible adverse effects on plants, underscoring the need for ecologically responsible disposal of graphene and for more research on the potential effects of graphene on agricultural and environmental systems.

3.1. *Graphene analysis*

Water-soluble graphene, commonly referred as graphene oxide with sodium ions as the counterions (solution pH 6.32), was used throughout this study. AFM was used to evaluate the morphologies of the graphene; Fig. 1 shows typical AFM images. The apparent heights of all the graphene observed were found to be around 1 nm, indicating that the graphene was fully exfoliated into individual sheets with the size of length × breadth ranged from 0.5 × 0.6 ~ 1.5 × 6.5 μm for 30 pieces of the graphene. Fig. 2a shows

typical SEM image of the graphene, revealing the morphology of the graphene sheets. Fig. 2b shows a TEM image of the graphene, which exhibits a typical wrinkled structure [33] with the corrugation and scrolling that are fundamental to graphene [34].

Fig. 1 here

Fig. 2 here

3.2. *Graphene repression of plant growth*

We conducted a series of tests of the potential effect of graphene on the growth of tomato, cabbage, red spinach, and lettuce. Treated and untreated seeds were germinated after 4 days of incubation at 25 °C in the dark. Fully germinated seedlings with developed cotyledons and root system are shown in Fig. 3. Cotyledons and root system were retarded with increasing graphene concentration. Only in the case of lettuce was there no significant influence of graphene on the cotyledons and root system after 4 days (data not shown). On the other hand, graphene had a clear negative influence after 20 days on root and shoot length and biomass of tomato, cabbage and red spinach exposed to graphene. The observed influence depended on the concentration of graphene and the duration of the experiment. In hydroponics experiments, when plants were treated with different concentrations of graphene (0, 500, 1000, and 2000 mg/L), the 20-day-old plants were characterized by inhibition of plant growth and leaf number and leaf size decreased with increasing graphene concentration in comparison with control (Fig. 4) and showed toxicity symptoms. As can be seen in Fig. 3 and 4, the primary roots were much shorter and the root hairs almost disappeared for plants treated with 2000 mg/L and as a result,

the overall amount of graphene aggregated on the surface of the roots was not in proportional to the graphene concentrations. Similar results were also observed for *Brassica juncea* and *Phaseolus mungo* plants treated with other types of the carbon nanoparticles [15]. Root tips and root hairs produce large amounts of mucilage, a highly hydrated polysaccharide coating on the root surface [35], which are the key species responsible for absorbing the nanoparticles onto the root surface. No significant effect of graphene on the parameters tested (seed germination and growth) was noted in our experiment in the case of lettuce. A certain species of plants responds in its very own manners to the nanoparticles. Difference in structures of the xylem would be the key physiological reason responsible for this fact. In the present studies, cabbage, tomato and red spinach contain one primary root and several smaller lateral roots, whereas lettuce has numerous small roots with a primary root. And as a result, no significant phytotoxicity of graphene on lettuce was observed compared to cabbage, tomato and red spinach. Canas and co-workers [36] described in their studies that the species would respond differently to nanomaterials, and responses among species did, in fact, vary. Lee *et al.* [37] also reported that nanoparticles toxicity depends on probably due to differences in root anatomy because xylem structures determine the speed of water transport and different xylem structures may demonstrate different uptake kinetics of nanoparticles [38]. The following discussion is focused on the results obtained for tomato, cabbage and red spinach.

Fig. 3 here

Fig. 4 here

The presence of graphene resulted in decreased root and shoot growth (Fig. 5a and b). However, graphene at a lower concentration (500 mg/L) resulted in only a slight decrease in root and shoot length. A marked inhibition effect was observed with the highest concentration of graphene (2000 mg/L). In the case of cabbage, there was a significant increase in root and shoot growth inhibition greater than 78% and 61%, respectively, compared to control. The 2000 mg/L concentration graphene resulted in root and shoot growth inhibition of tomato of 46% and 53%, respectively, compared to control. Inhibition of shoot growth was noted in red spinach (13%) at 500 mg/L, and the highest concentration (2000 mg/L) resulted in further significant inhibition of shoot growth (39%). However, no significant effect of graphene on the root growth of red spinach at 500 mg/L was observed while root growth of red spinach was inhibited by 18% at the higher graphene concentrations (1000 and 2000 mg/L).

Fig. 5 here

The presence of graphene resulted in decreased root and shoot weight (Fig. 5c and d). With cabbage seedlings grown in hydroponic culture, the root and shoot weight was sensitive to graphene, and weight decreased by 88% and 81%, respectively, at the highest concentration (2000 mg/L) compared to control. The root and shoot weight of tomato was also sensitive to graphene, and weight decreased by 86% and 92%, respectively, at the highest concentration (2000 mg/L) compared to control. With red spinach, the shoot weight appeared to be more sensitive to graphene compared to root; the root and shoot

weight of red spinach decreased by 39% and 75% at the highest concentration (2000 mg/L), respectively, compared to control. Tomato seedlings were somewhat more sensitive to graphene than were cabbage and red spinach seedlings.

Graphene influenced the leaves of all tested plants in a dose-dependent manner (Fig. 5e). The number of leaves decreased with increasing graphene concentration compared with control. For example, control tomato without graphene developed an average of 17 leaves each, whereas the treated tomato developed only 8 leaves each at 1000 and 2000 mg/L (Fig. 5e). The leaf numbers of the treated plants were considerably decreased by 40%, 53%, and 33% at the highest graphene concentration (2000 mg/L) in cabbage, tomato, and red spinach, respectively. The leaves exhibited reduced size and wilting symptoms, as evidenced by visual observation (Fig. 4). Of interest, the leaf area (visual observation, Fig. 4, Fig. 5f) of all treated plants was gradually reduced and continued to decline with increasing graphene level. A significantly reduced leaf area of the treated plants was clearly observed at graphene concentration (2000 mg/L, Fig. 5f) compared to control. Furthermore, the leaf area of cabbage was reduced by 25% at 500 mg/L and by 71% at 2000 mg/L compared to control, indicating a dose-dependent reduction. Tomato had an 88% leaf area reduction at 2000 mg/L (Fig. 5f) and 45% at 500 mg/L. The leaf area of red spinach was reduced by 91% at 2000 mg/L compared to control (Fig. 5f).

We found that cotyledons and the root system of cabbage, tomato, and red spinach were inhibited after four days and observed further inhibition in seedling growth at different graphene concentrations. Although 500 mg/L graphene had a slight effect, 2000 mg/L resulted in a notable effect on the seedling stage of cabbage, tomato, and red spinach. By comparison, graphene at 50 μg⁄mL increased growth rates with no sign of

significant toxicity for tomato in the seedling stage [13]. Khodakovskaya *et al*. [13] investigated the effect of four carbon materials (single- multiwall carbon nanotubes, few-layer graphene, and activated carbon) on the seedling stage of tomato at 50 μg⁄mL. As noted, a high concentration of graphene was not employed in that study, and the authors used only one low concentration.

3.3. *ROS measurements and H_2O_2 detection*

Plants continuously produce ROS as byproducts of various metabolic pathways, but the excess accumulation of ROS leads to oxidative stress and cell death [39, 40]. ROS products, whether inside or outside the cell, can be key factors in the toxicological effects of nanostructure materials [12]. Carbon nanotubes (CNTs) are known to have phytotoxic effects in plant cells because of aggregation [25], causing cell death and accumulated ROS in a dose-dependent manner [41]. Graphene may have the ability to generate ROS production, based on the similarities of some of the properties of graphene sheets of CNTs. Based on the assumption that graphene can be involved in ROS production in the leaf, we tested this possibility using 20-day-old leaves from test plants for the detection of ROS by means of the ROS-sensitive dye DCFH-DA.

We evaluated ROS accumulation (oxidative stress) by means of H_2O_2 detection after infiltration with DCFH-DA of treated and untreated leaves. The accumulation of H_2O_2 was visualized under a microscope; it can be imaged under fluorescence microscopy after removal of DCFH-DA from the leaves by washing with PBS buffer (Fig. 6a–f). Fig. panels 6b, 6d, and 6f illustrate that graphene-treated leaves showed an increase in DCFH fluorescence compared to control leaves (Fig. 6a, c, and e) of cabbage, tomato, and red

spinach, respectively. Measurement of DCFH fluorescence by spectrofluorometer demonstrated the dose-dependent increase in ROS content in graphene-treated leaves (Fig. 6g) compared to control. The accumulation of ROS in the leaf was measured with the excitation wavelength at 485 nm and emission wavelength at 522 nm. As Fig. 6g shows, as the concentration of graphene in medium increased, a progressively enhanced DCFH response was observed, strongly suggesting that graphene can cause an oxidative stress reaction in plant cells.

As Fig. 6g shows, in the case of red spinach, graphene and the control without graphene shared similar fluorescence intensity, specifically at the low graphene concentration (500 mg/L). This finding supports that a low concentration of graphene is not responsible for induction of ROS. In contrast, graphene at a high concentration elicited a sharply increased ROS level compared to control.

Fig. 6 here

We further tested the ROS accumulation induced by graphene in 20-day-old leaves of cabbage, tomato, and red spinach by means of the ROS-sensitive dye DAB. Infiltration of leaves with DAB allowed the detection of H_2O_2. The location of insoluble deep radish brown polymerization product produced when DAB reacts with H_2O_2 was visualized under a light microscope; it can be imaged after removal of chlorophyll from the leaves by boiling for 15 min in ethanol. Imaging of deep radish brown polymerization can be considered to indicate the accumulation of H_2O_2 (Fig. 7b, d and f) in cabbage, tomato, and red spinach, respectively, and formation of H_2O_2 would be expected as a result of the

ROS accumulation by graphene induction. In control leaf (Fig. 7a, c and e) of cabbage, tomato, and red spinach, respectively, no distinctive deep radish brown polymerization of H_2O_2 was detectable. The plants exposed to concentrations of 1000 mg/L showed significant toxicity after 20 days, with the DAB assay indicating increasing ROS. The amount of formazan formation in leaves was determined at A_{700}. As shown in Fig. 7g, higher levels of graphene (1000 mg/L) triggered production of more ROS. The excess ROS production at 1000 mg/L may be indicative of concentration-dependent ROS generation.

Fig. 7 here

ROS production estimated by DCF-DA was correlated to an increase in ROS predictable by DAB assays. However, the results of both assays demonstrated the direct presence of ROS that are produced inside the leaf in those plants grown with graphene. The ROS localization using DCFH-DA and DAB described above was also supported by the quantitative determinations of DCFH and deep brown polymerization at a higher concentration of graphene (1000 mg/L) (Fig. 6g and Fig. 7g). These findings are in agreement with those of Zhang *et al*. [18], who exposed neural pheochromocytoma-derived PC12 cells to graphene and demonstrated that graphene-induced ROS were involved in the toxic mechanism. In fact, ROS are the key signaling molecules and could be induced by many exogenous stimuli [39].

Evidence for the accumulation of ROS induced by graphene includes that the ability of graphene to reduce plant growth was positively correlated with the generation of ROS

with graphene concentration in a dose-dependent manner, as was estimated by DCFH-DA. In previous studies, graphene was found to be also capable of generating ROS to A549 cells, a typically adenocarcinomic human alveolar basal epithelial cell line [42,18]. The ROS induced oxidative stress is considered to be the common toxicological mechanism of the nanoparticles [43-46]. Graphene obtained using Hummer's method was seen to be electron paramagnetic resonance active (EPR-active) with ~1016 electron spins/g [47]. Graphene catalyzes the generation of ROS to plants (cabbage, tomato, and red spinach) once it has been covering on the roots of plants.

3.4. *Evaluation of cell death*

To evaluate the toxicity of graphene through cell membrane damage *in vivo* in hydroponic culture conditions, we used a cell death assay. The roots of treated and untreated seedlings were examined by measuring cell death using Evans blue staining and with O.D. values at 597 nm after a 20-day exposure to different concentrations (0, 500, 1000, and 2000 mg/L) of graphene. The measurement of the Evans blue extracted from roots showed a concentration-dependent induction (Fig. 8a). With the concentration of graphene increasing to 1000 and 2000 mg/L in the case of cabbage, the amount of Evans blue uptake in root cells increased by about 5 and 12.3 fold, respectively, compared to that of control roots. A significant level of Evans blue uptake was observed after both 1000 and 2000 mg/L of graphene treatment of tomato roots, representing 11.5 and 14.4 fold, respectively, of that in control roots. The higher concentrations of graphene (1000 and 2000 mg/L) caused 8.5- and 11.8-fold higher uptake, respectively, of Evans blue in roots of red spinach compared to that in control roots. Thus, these results indicate that the

loss of plasma membrane integrity occurred with exposure to graphene, as it was greater than in the control plants. Higher (1000 and 2000 mg/L) graphene concentrations caused severe stress on plant growth, inducing the excess generation of ROS. The effects of the ROS may be reflected in the rapid rise of Evans blue uptake. The toxic effect on plant roots appeared after exposure to the lower concentration of graphene, and differences between controls and graphene-treated plants became even more prominent at higher concentrations of graphene, as observed under a light microscope (data not shown).

Fig. 8 here

We analyzed another cell death index to further demonstrate that graphene causes cell membrane damage (electrolyte leakage/plasma membrane sensitivity) in the treated leaf. Electrolyte leakage experiments indicated that the leaves of the graphene-treated plants had decreased membrane integrity (Fig. 8b). For these experiments, we used 20-day-old seedlings with leaves, investigating the effect of increasing concentrations of graphene on membrane integrity. Cell membrane damage was noted at 500 mg/L in cabbage, tomato, and red spinach, and 1000 and 2000 mg/L resulted in further damage, indicating dose-dependent membrane integrity and disruption of the plasma membrane. In addition, as shown in Fig. 8b, the results of the electrolyte leakage experiments indicated that the tomato had significantly greater leakage at the highest concentration (2000 mg/L) compared to cabbage and red spinach. A comparison of Fig. 8a and b shows that enhancement of Evans blue uptake and loss of plasma membrane integrity gradually increased up to 2000 mg/L graphene under the same conditions. Evans blue staining

showed that extensive cell death/membrane injury was induced in plant roots by different concentrations of graphene treatment. The electrolyte leakage assay confirmed the membrane injury resulting from graphene treatment. This result indicates that the loss of plasma membrane integrity was induced by graphene at the lower concentration and continued at higher concentrations. These results also suggest that intracellular ROS might have a crucial role in induction of cell death induced by graphene. It has been reported that the accumulation of ROS causes cell death, which is demonstrated by electrolyte leakage from cells [48].

The effect of graphene on cell death was evaluated by Evans blue staining and a conductivity method (% of membrane leakage). These two assays have been considered as indexes of cell death in plants [49], although they give information only about plasma membrane integrity. The Evans blue assay is based on the accumulation of blue color inside dead cells (but not in living cells). The conductivity assay is based on electrolyte leakage from dying cells, with ion leakage used as a marker of cell death.

3.5. *Morphological observation by SEM*

To provide clues to graphene toxicity in the seedling stage of terrestrial plant roots, we next visualized the morphological alteration of cabbage, tomato, and red spinach using SEM of the treated roots and compared them to untreated controls (Figs. 9, 10, and 11, respectively). SEM examination of the tested plants exposed to a higher concentration of graphene (1000 mg/L) revealed several morphological alterations compared to the control plants grown in Hoagland medium. At 20 days without exposure to graphene, the majority of the root surface appeared healthy; little to no alteration in morphology was

observed. Regarding morphology at 1000 mg/L of graphene, root shape changed especially above the elongation area of cabbage and tomato (Fig. 9 and Fig. 10, respectively) compared to control. Epidermis of the treated tomato (Fig. 10b, c, e and f) and red spinach (Fig. 11b, d and e) root was loosely detached or even completely detached compared to control, which was characteristic for membrane damage as determined by Evans blue. We note that specific differences could be observed after Evans blue staining at the light microscopic level (data not shown) with respect to the cell morphology between roots exposed to different concentrations of graphene. Thus, differences in cell death determined from Evans blue assays do reflect the sensitivity of cells to different concentrations of graphene, although the morphological alterations observed from light microscopy indicate a common cell death pathway. These results imply that the root membrane with a higher graphene concentration (1000 mg/L) had no tolerance to graphene stress. An aggregation of graphene was noted on the surface of the root of cabbage, tomato, and red spinach, indicating that aggregation of graphene contributes at least in part to its toxic properties, as is the case for CNTs [21]. Uptake, translocation, and accumulation of CNTs in roots and leaves were reported for tomato [13]. In our studies with graphene as the typical carbon nanoparticles, insights into the penetration, translocation, and/or accumulation of graphene into the intracellular locations were not observed for all of the four species (cabbage, tomato, red spinach, and lettuce). This was confirmed by observing the plant specimens by TEM during the courses of the plant incubation.

The root surface area of the graphene-treated cabbage was different from the untreated control (Fig. 9). The root surface area of cabbage was significantly increased by graphene

treatment, and it may be that an excess of graphene resulted in swelling. This observation is similar to results previously reported for *Origanum vulgare* by Panou-Filotheou and Bosabalidis [50] and in cowpea by Kopittke *et al*. [51]. At a higher graphene concentration (1000 mg/L), the root hair growth of cabbage and red spinach was significantly decreased compared to control.

Fig. 9, 10, and 11 here

The two forms of carbon nanoparticles, CNTs and graphene, have similar chemical composition and crystalline structure. Based on this fact, a reasonable inference is that the two would be similar in many ways, such as biological activity. But they are different in shape; CNTs are tubular while graphene is flat atomic sheets [52]. As a result, atomically flat graphene nanostructures have been estimated to have an even stronger interaction with biological systems than the tubular-shaped CNTs. There is evidence that CNTs could translocate to systemic sites (roots, leaves, and fruits) and engage in a strong interaction with the cells of tomato seedlings, resulting in significant changes in total gene expression in roots, leaves, and fruits [13] and exerting toxic effects [15,16,26]. CNTs are also known to have phytotoxic effects in plant cells because of aggregation [25], causing cell death and accumulated ROS in a dose-dependent manner [41]. Considering these aspects, it is not unexpected to find toxic effects of graphene on terrestrial plant species, as we did in tomato, cabbage, and red spinach in the current study. Oxidative stress has been regarded as a suitable mechanism for explaining the toxicity of graphene.

The phytotoxicity of graphene is likely the result of its ability to generate ROS as represented predominantly by H_2O_2 using the ROS-sensitive dyes DCFH-DA and DAB. Reports regarding graphene-induced oxidative stress are available [18]. Concerning the relationship between graphene-mediated ROS generation and cell death in plants, we investigated physiological and morphological endpoints, including visual symptoms, ROS production, SEM observation, and cell death–related responses after exposure to graphene for 20 days. Graphene-treated leaves showed significant accumulation of H_2O_2 compared with control (Fig. 6). This observation was closely associated with visible signs of necrotic damage lesions (Fig. 4), cellular ROS accumulation monitored by DAB (Fig. 7), and membrane damage (Fig. 8b). The evidence of massive cell death (electrolyte leakage assay) as well as visual signs (Fig. 4 and Fig. 7) with the graphene-treated leaves demonstrated that at 20 days following exposure to graphene, necrosis was the predominant death response in treated leaf cells. In addition, the spatial pattern of H_2O_2 production was mainly located in the close proximity of visible symptomatic areas and the sites undergoing cell death.

Plant cell death occurs either by apoptosis or by necrosis. Necrosis is passive and characterized by a progressive loss of membrane integrity that results in cytoplasmic swelling and release of cellular constituents [53]. Furthermore, we also detected the effect of graphene on the morphology of roots, finding that the epidermis of the treated tomato and red spinach roots was loosely detached or even completely detached. Further, the aggregation of graphene was noted on the surface of the roots of all graphene (1000 mg/L)-treated plants, indicating that aggregation of graphene contributed at least in part to its toxic properties, as is the case for CNTs [25]. On the basis of these results, we infer

that graphene phytotoxicity involved the oxidative stress mechanism mediated through the necrotic pathway. In biological systems, ROS production and disturbances of cellular redox potentials have been found to be involved either directly or indirectly in the death of individual cells and/or the development of necrotic lesions [54, 55]. Enhanced generation of ROS (hydrogen peroxide) and plasma membrane rupture have been traditionally associated with pathogenic events including necrotic cell death, which is recognized by morphological signs and is usually considered to be uncontrolled [56].

4. Conclusions

In summary, we showed that graphene exerted toxic effects on terrestrial plant species such as cabbage, tomato, and red spinach. The overproduction of ROS induced by graphene could be responsible for significant plant growth inhibition and biomass reduction compared to control. Nel *et al*. [12] reported that the production of ROS can be a key factor in the toxicological effects of nanostructure materials. Observation of accumulation ROS production by means of H_2O_2 visualization along with visible signs of necrotic damage lesions and evidence of a massive electrolyte leakage all indicated an oxidative stress mechanism mediated through the necrotic pathway, which requires further study. We suggest an evaluation of graphene toxicity to targets on terrestrial plant species and applying a prolonged exposure period with different concentrations to measure any potential risk.

Acknowledgments

We gratefully acknowledge Prof. Toru Mura and Prof. Shunitz Tanaka for providing necessary facilities during the study. We also gratefully acknowledge Yoshinobu Nodasaka and Natsumi Ushijima for their kind assistance in preparing the SEM and TEM samples. Many thanks go to Hongwen Yu for his assistance during the AFM study. The very helpful comments from the reviewers on the preliminary version of this paper are also gratefully acknowledged.

REFERENCES

[1] Joseph T, Morrison M. Nanotechnology in Agriculture and Food. 2006. Available from:http://www.nanoforum.org/datein/temp/nanotechnology%20in%20agriculture%20and%food.pdf?08122006200524

[2] Geim AK, Novoselov KS. The rise of graphene. Nat Mater 2007;6(3):183–91.

[3] Ando T. The electronic properties of graphene and carbon nanotubes. NPG Asia Mater 2009;1(1):17–21.

[4] Xia J, Chen F, Li J, Tao N. Measurement of the quantum capacitance of graphene. *Nat Nanotech* 2009;4:505–509.

[5] Enderlein C, Kim YS, Bostwick A, Rotenberg E, Horn K. The formation of an energy gap in graphene on ruthenium by controlling the interface. New J Phys 2010;12:033014 (9pp).

[6] Dragoman M, Dragoman D. Graphene-based quantum electronics. Prog Quantum Electron 2009;33(6):165-214.

[7] Monica RC, Cremonini R. Nanoparticles and higher plants. Caryologia 2009;62(2):161-165.

[8] Bhabra G, Sood A, Fisher B, Cartwright L, Saunders M, Evans WH, et al. Nanoparticles can cause DNA damage across a cellular barrier. Nat Nanotech 2009;4:876-883.

[9] Nowack B, Bucheli TD. Occurrence, behavior and effects of nanoparticles in the environment. Environ Pollut 2007;150(1):5–22.

[10] Kirchner C, Liedl T, Kudera S, Pellegrino T, Javier AM, Gaub HE, et al. Cytotoxicity of colloidal CdSe and CdSe/ZnS nanoparticles. Nano Lett 2005;5(2):331–338.

[11] Jia G, Wang H, Yan L, Wang X, Pei R, Yan T, et al. Cytotoxicity of carbon nanomaterials: single-wall nanotube, multi-wall nanotube, and fullerene. Environ Sci Tech 2005;39(5):1378–1383.

[12] Nel A, Xia T, Madler L, Li N. Toxic potential of materials at the nanolevel. Science 2006;311(5761):622-627.

[13] Khodakovskaya MV, Silvaa Kde, Nedosekinb DA, Dervishic E, Birisa AS, Shashkovb EV, et al. Complex genetic, photothermal, and photoacoustic analysis of nanoparticle-plant interactions. PNAS 2011;108(3):1028–1033.

[14] Liu Q, Chen B, Wang Q, Shi X, Xiao Z, Lin J, et al. Carbon nanotubes as molecular transporters for walled plant cells. Nano Lett 2009;9(3):1007–1010.

[15] Ghodake G, Seo YD, Park D, Lee S. Phytotoxicity of carbon nanotubes assessed by *Brassica Juncea* and *Phaseolus Mungo.* J Nanoelectron and Optoelectron 2010;5(2):157-160.

[16] Stampoulis D, Sinha SK, White JC. Assay-dependent phytotoxicity of nanoparticles to plants. Environ Sci Tech 2009;43(24):9473-9479.

[17] Lin DH, Xing BS. Phytotoxicity of nanoparticles: inhibition of seed germination and root growth. Environ Pollut 2007;50(2):243-250.

[18] Zhang Y, Ali SF, Dervishi E, Xu Yang, Li Z, Casciano D, et al. Cytotoxicity effects of graphene and single-wall carbon nanotubes in neural Phaeochromocytoma-derived PC12 Cells. ACS Nano 2010;4(6):3181-3186.

[19] Akhavan O, Ghaderi E. Toxicity of graphene and graphene oxide nanowalls against bacteria. ACS Nano 2010;4 (10):5731–5736.

[20] USEPA-Ecological Effects Test Guidelines (OPPTS 850.4200) Seed germination root elongation toxicity test. 1996. Available from: http://www.epa.gov/opptsfrs/publications/OPPTS_Harmonized/850_Ecological_Effects_Test_Guidelines/Drafts/850-4200.pdf

[21] Rico MC, Majumdar S, Duarte-Gardea M, Peralta-Videa RJ, Gardea-Torresdey LJ. Interaction of nanoparticles with edible plants and their possible implications in the food chain. J Agric Food Chem 2011;59 (8):3485–3498.

[22] El-Temsah Y S, Joner E J. Impact of Fe and Ag nanoparticles on seed germination and differences in bioavailability during exposure in aqueous suspension and soil. Environ Toxicol 2010.

[23] Lopez-Moreno ML, De La Rosa G, Hernandez-Viezcas JA, Peralta-Videa JR, Gardea-Torresdey JL. X-ray absorption spectroscopy (XAS) corroboration of the uptake and storage of CeO_2 nanoparticles and assessment of their differential toxicity in four edible plant species. J Agric Food Chem 2010; 58:3689– 3693.

[24] Sayes CM, Liang F, Hudson JL, Mendez J, Guo W, Beach JM, et al. Functionalization density dependence of single-walled carbon nanotubes cytotoxicity *in Vitro*. Toxicol Lett 2006;161:135–142.

[25] Lin C, Fugetsu B, Su Y, Watari F. Studies on toxicity of multi-walled carbon nanotubes on *Arabidopsis* T87 suspension cells. J Hazard Mater 2009;170(2-3): 578-583.

[26] Lin S, Reppert J, Hu Q, Hudson JAS, Reid ML, Ratnikova TA, et al Uptake, translocation, and transmission of carbon nanomaterials in rice plants. Small 2009;5(10):1128-1132.

[27] Hummers WSJr, Offeman RE. Preparation of graphitic oxide. J Am Chem Soc 1958;80(6):1339.

[28] Hoagland DR, Arnon DI. The water culture method for growing plants without soil. The College of Agriculture, University of California, California Agriculture Experiment Station Circular 347, Berkeley 1950:1-32.

[29] Murata MR, Hammes PS, Zharare GE. Effect of solution pH and calcium concentration on germination and early growth of groundnut. J Plant Nutr 2003;26:1247–1262.

[30] Thordal-Christensen H, Zhang Z, Wei Y, Collinge DB. Subcellular localization of H_2O_2 in plants. H_2O_2 accumulation in Papillae and hypersensitive response during the barley-powdery mildew interaction. Plant J 1997;11(6):1187–1194.

[31] Baker CJ, Mock NM. An improved method for monitoring cell death in cell suspension and leaf disc assays using Evans blue. Plant Cell, Tissue Organ Culture 1994;39(1):7–12.

[32] Lutts S, Kinet JM, Bouharmont J. NaCl-induced senescence in leaves of rice (*Oryza sativa* L.) cultivar differing in salinity resistance. Ann Bot (Lond) 1996;78(3):389–398.

[33] Stankovich S, Dikin DA, Dommett GHB, Kohlhaas KM, Zimney EJ, Stach EA, et al. Graphene-based composite materials. Nature 2006;442(7100):282-286.

[34] Meyer JC, Geim AK, Katsnelson MI, Novoselov KS, Booth TJ, Roth S. The structure of suspended graphene sheets. Nature 2007;446(7131):60-63.

[35] Campbell NA. Biology, 2nd ed. The Benjamin/Cummings Publishing Company: Redwood City, California 1990.

[36] Canas JE, Long M, Nations S, Vadan R, Dai L, Luo M, et al. Effects of functionalized and nonfunctionalized single-walled carbon-nanotubes on root elongation of select crop species. Nanomater Environ 2008; 27:1922– 1931.

[37] Lee CW, Mahendra S, Zodrow K, Li D, Tsai YC, Braam J, et al. Developmental phytotoxicity of metal oxide nanoparticles to *Arabidopsis thaliana*. Environ Toxicol Chem 2010;29 (3):669–675.

[38] Ma X, Geiser-Lee J, Deng Y, Kolmakov A. Interactions between engineered nanoparticles (ENPs) and plants: phytotoxicity, uptake and accumulation. Sci Total Environ 2010;408: 3053– 3061.

[39] Apel K, Hirt H. Reactive oxygen species: metabolism, oxidative stress, and signal transduction. Annu Rev Plant Biol 2004;55:373-399.

[40] Wen F, Xing D, Zhang LR. Hydrogen peroxide is involved in high blue light-induced chloroplast avoidance movements in *Arabidopsis.* J Exp Bot 2008;59(10):2891-2901.

[41] Tan XM, Lin C, Fugetsu B. Studies on toxicity of multi-walled carbon nanotubes on suspension rice cells. Carbon 2009;47(15):3479-3487.

[42] Chang Y, Yang ST, Liu JH, Dong E, Wang Y, Cao A, et al. *In vitro* toxicity evaluation of graphene oxide on A549 cells. *Toxicol Lett* 2011; 200:201– 210.

[43] Lewinski N, Colvin V, Drezek R. Cytotoxicity of nanoparticles. Small 2008;4:26–49.

[44] Li N, Xia T, Nel AE. The role of oxidative stress in ambient particulate matter-induced lung diseases and its implications in the toxicity of engineered nanoparticles. Free Radic Biol Med 2008;44:1689–1699.

[45] Yang ST, Wang X, Jia G, Gu Y, Wang T, Nie H et al. Long-term accumulation and low toxicity of single-walled carbon nanotubes in intravenously exposed mice. Toxicol Lett 2008;181;182–189.

[46] Pulskamp K, Diabaté S, Krug HF. Carbon nanotubes show no sign of acute toxicity but induce intracellular reactive oxygen species in dependence on contaminants. Toxicol Lett 2007;168:58–74.

[47] Ali F, Agarwal N, Nayak PK, Das R, Periasamy N. Chemical route to the formation of grapheme.Current Sceince 2009; 97 (5):683-685.

[48] Kawai-Yamada M, Ohori Y, Uchimiya H. Dissection of *Arabidopsis* Bax inhibitor-1 suppressing Bax-, hydrogen peroxide-, and salicylic acid-induced cell death. Plant Cell 2004;16:21–32.

[49] Del Pozo O, Lam E. Caspases and programmed cell death in the hypersensitive response of plants to pathogens. Curr Biol 1998;8(20):1129-1132.

[50] Panou-Filotheou H, Bosabalidis AM. Root structural aspects associated with copper toxicity in Oregano (*Origanum vulgare* subsp. *hirtum*). Plant Sci 2004;166(6):1497–1504.

[51] Kopittke PM, Asher CJ, Kopittke RA, Menzies NW. Toxic effects of Pb^{2+} on growth of Cowpea (*Vigna unguiculata*). Environ Pollut 2007;150(2):280–287.

[52] Lui CH, Liu L, Mak KF, Flynn GW, Heinz TF. Ultraflat graphene. Nature 2009;462:339-341.

[53] Breusegem FV, Dat JF. Reactive oxygen species in plant cell death. Plant Physiol 2006;141(2):384–390.

[54] Pellinen RI, Korhonen MS, Tauriainen AA, Palva ET, Kangasjärvi J. Hydrogen peroxide activates cell death and defense gene expression in Birch. Plant Physiol 2002;130:549–560.

[55] Yoda H, Yamaguchi Y, Sano H. Polyamine oxidase is one of the key elements for oxidative burst to induce programmed cell death in Tobacco cultured cells. Plant Physiol 2006;142:193–206.

[56] Golstein P, Kroemer G. Cell death by necrosis: towards a molecular definition. Trends in Biochem Sci 2007;32(1):37-43.

Captions for Figures

Fig. 1. AFM image of graphene.

Fig. 2. (a) SEM image and (b) TEM image of graphene.

Fig. 3. Graphene affected cotyledons and root systems. (a–c) Tomato, cabbage, and red spinach seeds after incubation with and without graphene solution on filter paper for 4 days, respectively.

Fig. 4. Effect of graphene on growth and development of cabbage, tomato, and red spinach seedlings. (a–c) Tomato, cabbage, and red spinach seedlings were hydroponically grown in Hoagland media for 20 days with and without graphene, respectively.

Fig. 5. Effect of graphene on growth and development of cabbage, tomato, and red spinach seedlings. Twenty-day-old seedlings growing on Hoagland media with graphene (0, 500, 1000, and 2000 mg/L) were used for all measurements. Error bars represent standard deviation. (a) Root length, (b) shoot length, (c) root weight, (d) shoot weight, (e) leaf number, and (f) leaf area.

Fig. 6. Effect of graphene on the generation of ROS in leaves tested by means of the ROS-sensitive dye DCFH-DA in cabbage, tomato, and red spinach seedlings. Twenty-day-old leaves treated with or without 1000 mg/L graphene were used for all measurements. Images were observed with fluorescence microscopy. Left lane (a), (c), and (e) cabbage, tomato, and red spinach leaves without graphene, respectively. Right lane (b), (d), and (f) cabbage, tomato, and red spinach leaves with graphene (1000 mg/L), respectively. The green signal indicates ROS generation (DCFH fluorescence) in the graphene-treated leaves (4×). (g) Dose-related effects of graphene on ROS in treated leaves measured by DCFH fluorescence.

Fig. 7. Effect of graphene on accumulation of H_2O_2 in leaves tested by means of the ROS-sensitive dye DAB of cabbage, tomato, and red spinach seedlings. Twenty-day-old fresh leaves treated with or without 1000 mg/L graphene were used for all measurements. Left lane (a), (c), and (e) cabbage, tomato, and red spinach leaves without graphene, respectively. Right lane (b), (d), and (f) cabbage, tomato, and red spinach leaves with graphene (1000 mg/L), respectively. The brown staining indicates the formation of a brown polymerization product when H_2O_2 reacts with DAB, and viewed with light microscopy. (g) Effect of graphene (1000 mg/L) on accumulation of H_2O_2 in treated leaves as measured using DAB.

Fig. 8. Effect of graphene on cell death of cabbage, tomato, and red spinach seedlings. Twenty-day-old seedlings growing on Hoagland media with graphene (0, 500, 1000, and 2000 mg/L) were used for all measurements. Error bars represent standard deviation. (a) Cell death determined by Evans blue and (b) cell death determined by electrolyte leakage.

Fig. 9. Behavior of graphene (1000 mg/L) on the root surface of cabbage seedlings grown in Hoagland medium. (a, c, e) SEM image of the untreated control of cabbage root elongation, root hair zone and surface respectively. (b, d, f) SEM image of the graphene treated cabbage root elongation, root hair zone and surface respectively showing aggregates of graphene. Scale bars in (a, b) indicate 200 μm; in (c, d) 120 μm and in (e, f) 30.0 μm, respectively.

Fig. 10. Behavior of graphene (1000 mg/L) on the root surface of tomato seedlings grown in Hoagland medium. (a, d) SEM image of the untreated control of tomato root elongation and root hair zone respectively. (b) Root elongation zone of tomato root and (c,

e, f) showing surface detachment and aggregates of graphene on the tomato roots surface treated with graphene. Scale bars in (a, b) indicate 200 μm; in (c) 30.0 μm; in (d, e) 120 μm; and in (f) 15.0 μm, respectively.

Fig. 11. Behavior of graphene (1000 mg/L) on the root surface of red spinach seedlings grown in Hoagland medium. (a, c) SEM image of the untreated control of red spinach root elongation, root hair zone and surface respectively. (b) Root elongation zone showing root damage (d) root hair zone and (e) surface showing aggregates of graphene on the root of red spinach. Scale bar in (a) indicates 150 μm; in (b, c) 200 μm; in (d) 120 μm and in (e) 15.0 μm, respectively.

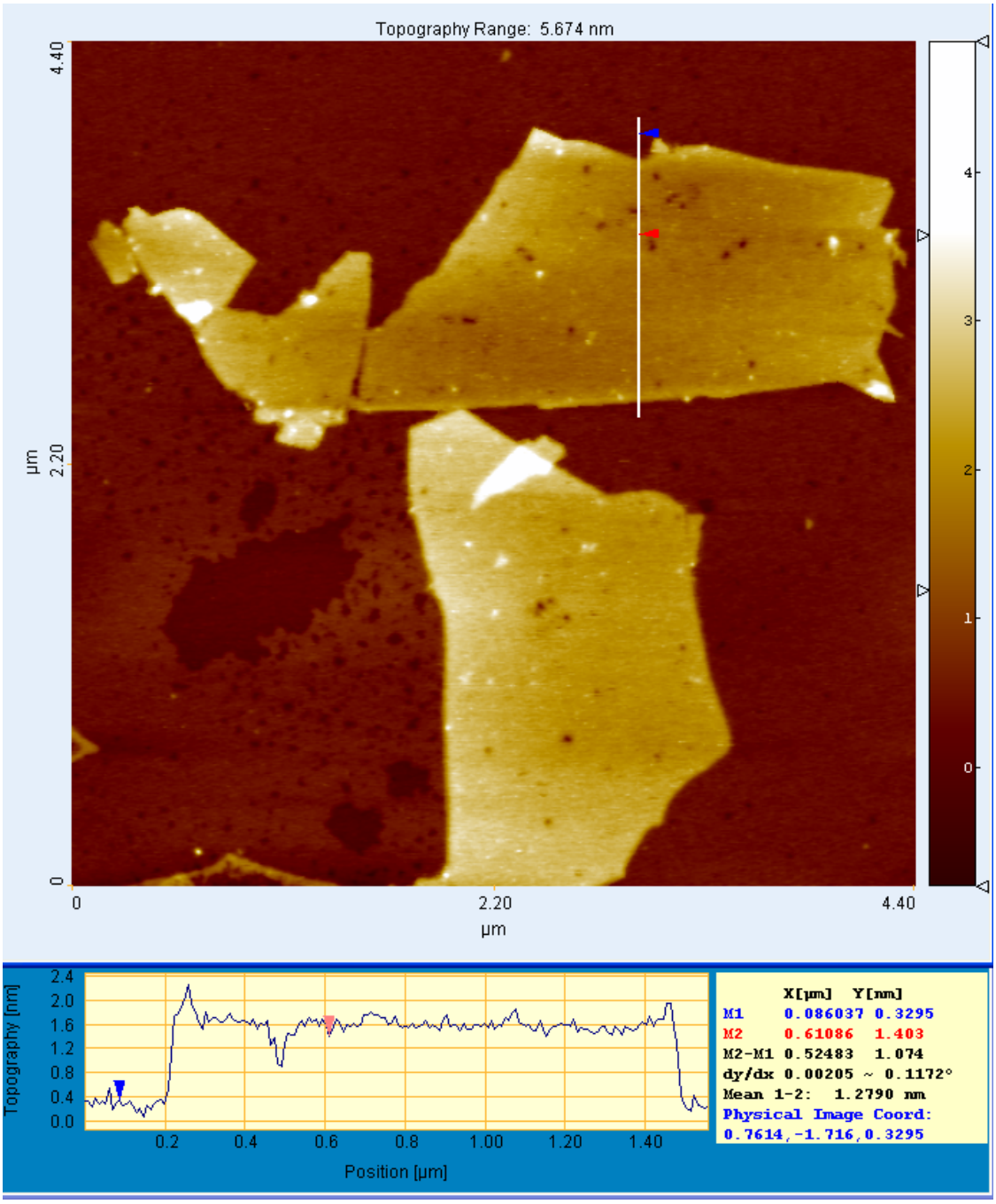
Topography Range: 5.674 nm
4.40
2.20
0
µm
0
2.20
4.40
µm
4
3
2
1
0
Topography [nm]
2.4
2.0
1.6
1.2
0.8
0.4
0.0
0.2
0.4
0.6
0.8
1.00
1.20
1.40
Position [µm]
X[µm] Y[nm]
M1 0.086037 0.3295
M2 0.61086 1.403
M2-M1 0.52483 1.074
dy/dx 0.00205 ~ 0.1172°
Mean 1-2: 1.2790 nm
Physical Image Coord:
0.7614,-1.716,0.3295

Fig. 1

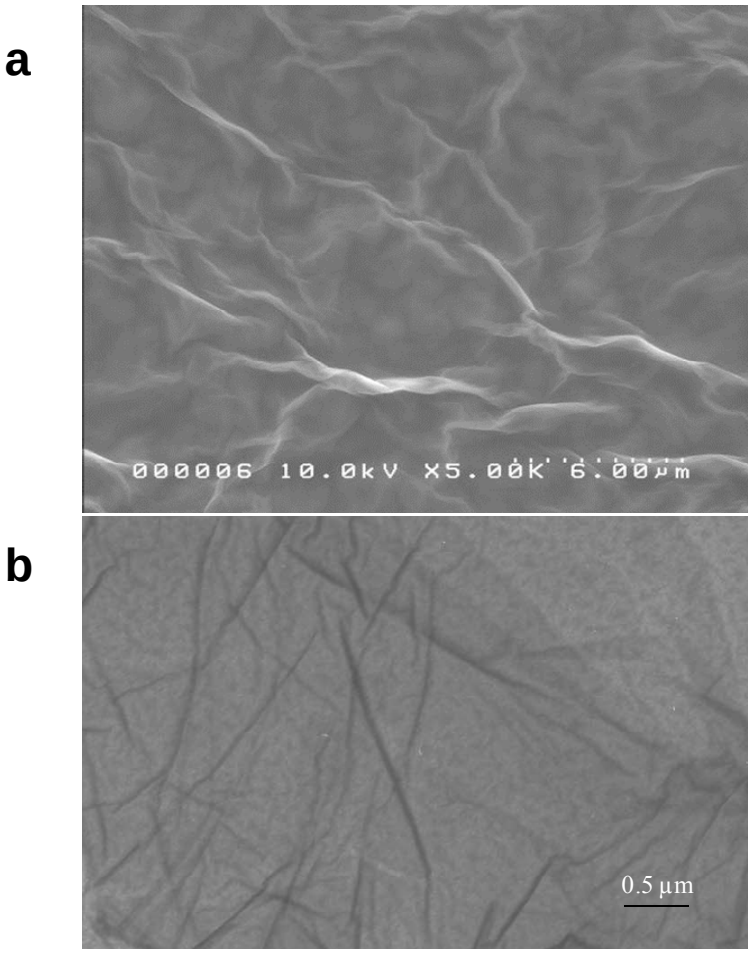

Fig. 2

(a)

0 500 1000 2000 (mg/L)

Concentration of graphene in growth medium

(b)

0 500 1000 2000 (mg/L)

Concentration of graphene in growth medium

(c)

0 500 1000 2000 (mg/L)

Concentration of graphene in growth medium

Fig. 3

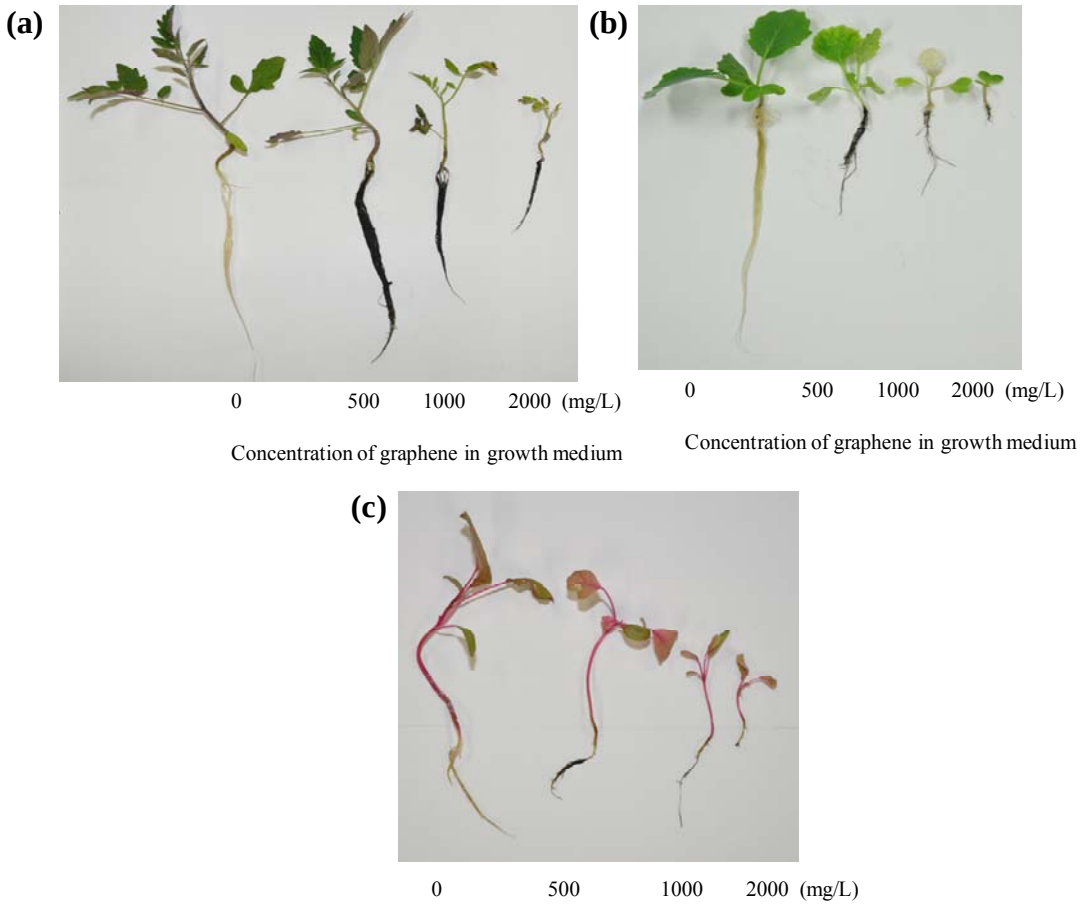
(a)
0 500 1000 2000 (mg/L)
Concentration of graphene in growth medium
(b)
0 500 1000 2000 (mg/L)
Concentration of graphene in growth medium
(c)
0 500 1000 2000 (mg/L)
Concentration of graphene in growth medium

Fig. 4

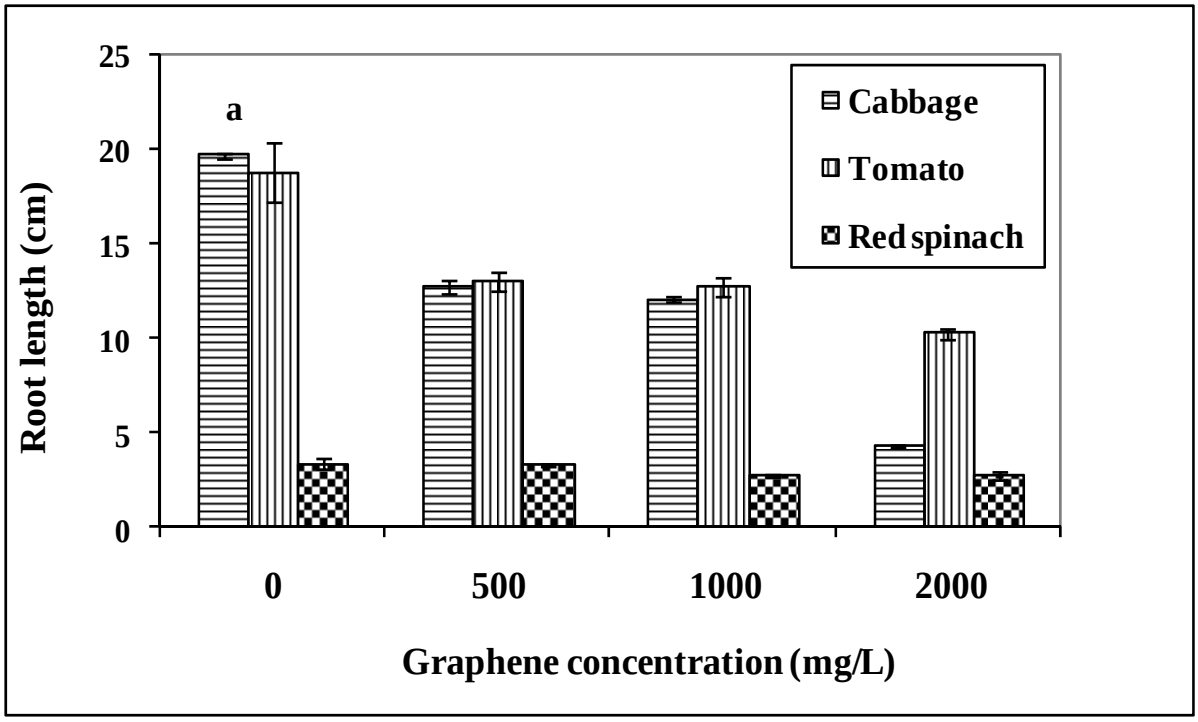
a
Root length (cm)
25
20
15
10
5
0
Cabbage
Tomato
Red spinach
0
500
1000
2000
Graphene concentration (mg/L)

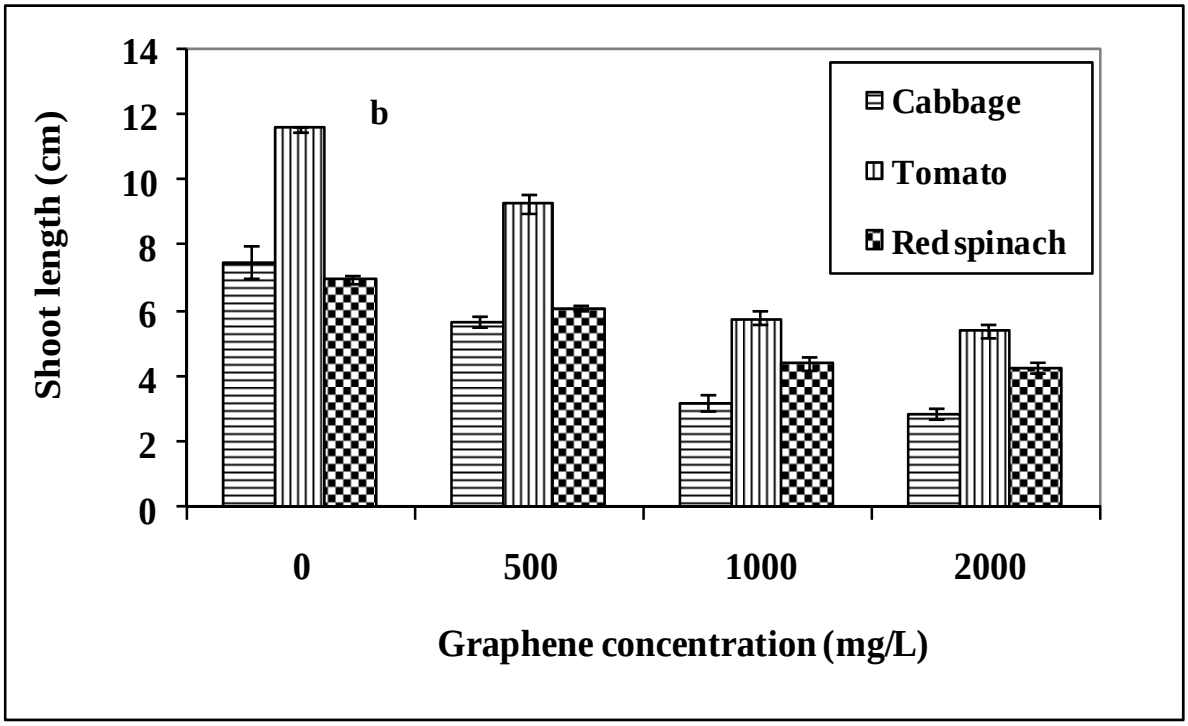
b
Shoot length (cm)
14
12
10
8
6
4
2
0
Cabbage
Tomato
Red spinach
0
500
1000
2000
Graphene concentration (mg/L)

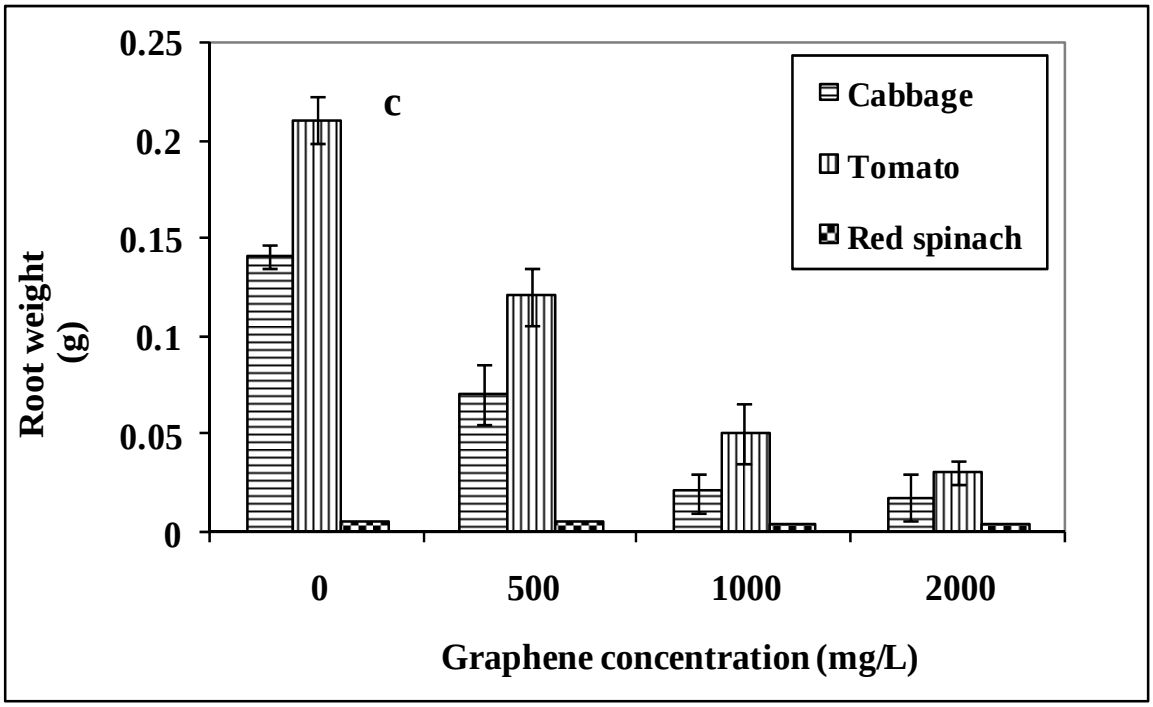
c
Root weight (g)
0.25
0.2
0.15
0.1
0.05
0
Cabbage
Tomato
Red spinach
0
500
1000
2000
Graphene concentration (mg/L)

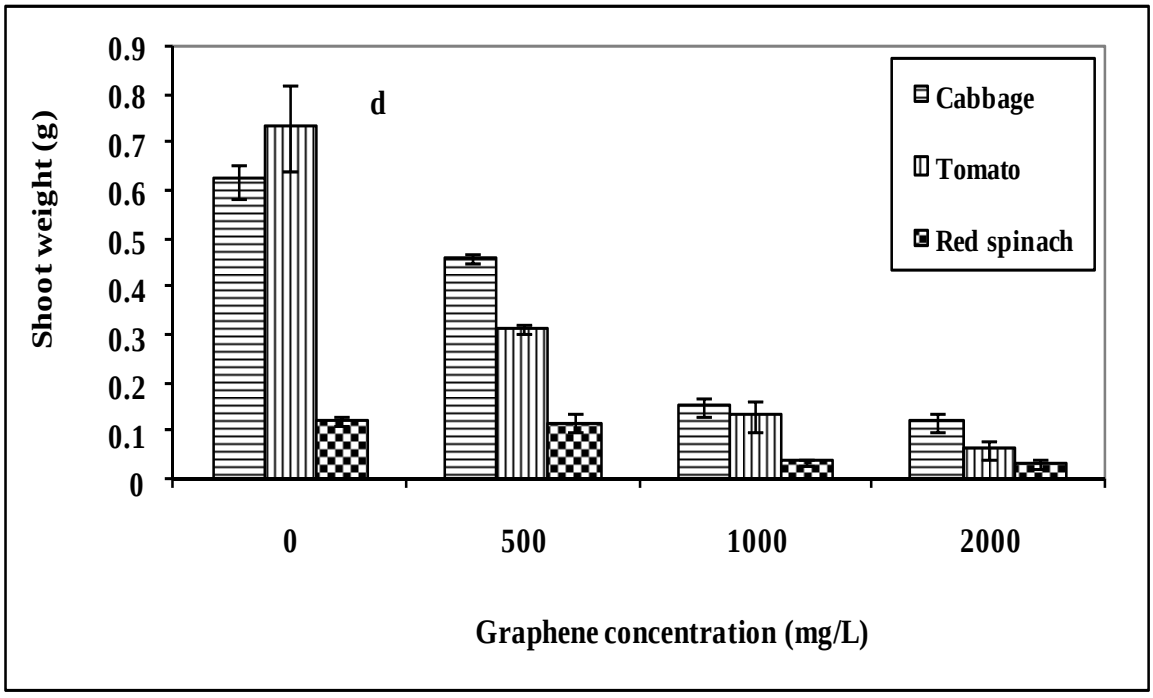
d
Shoot weight (g)
0.9
0.8
0.7
0.6
0.5
0.4
0.3
0.2
0.1
0
Cabbage
Tomato
Red spinach
0
500
1000
2000
Graphene concentration (mg/L)

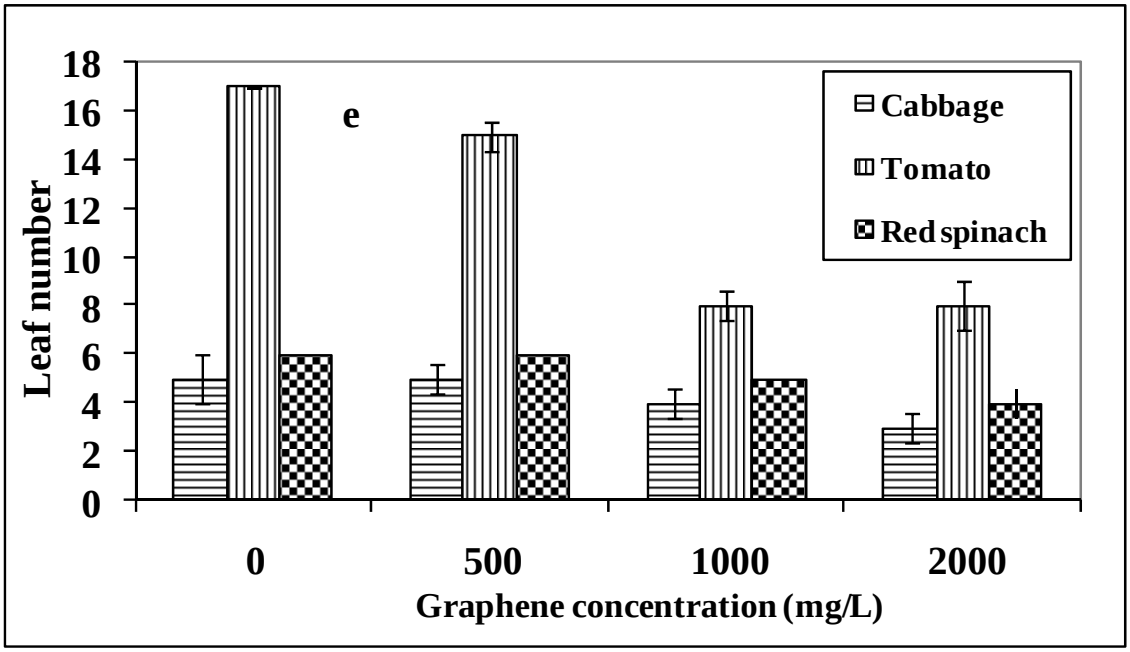
e
Leaf number
18
16
14
12
10
8
6
4
2
0
Cabbage
Tomato
Red spinach
0
500
1000
2000
Graphene concentration (mg/L)

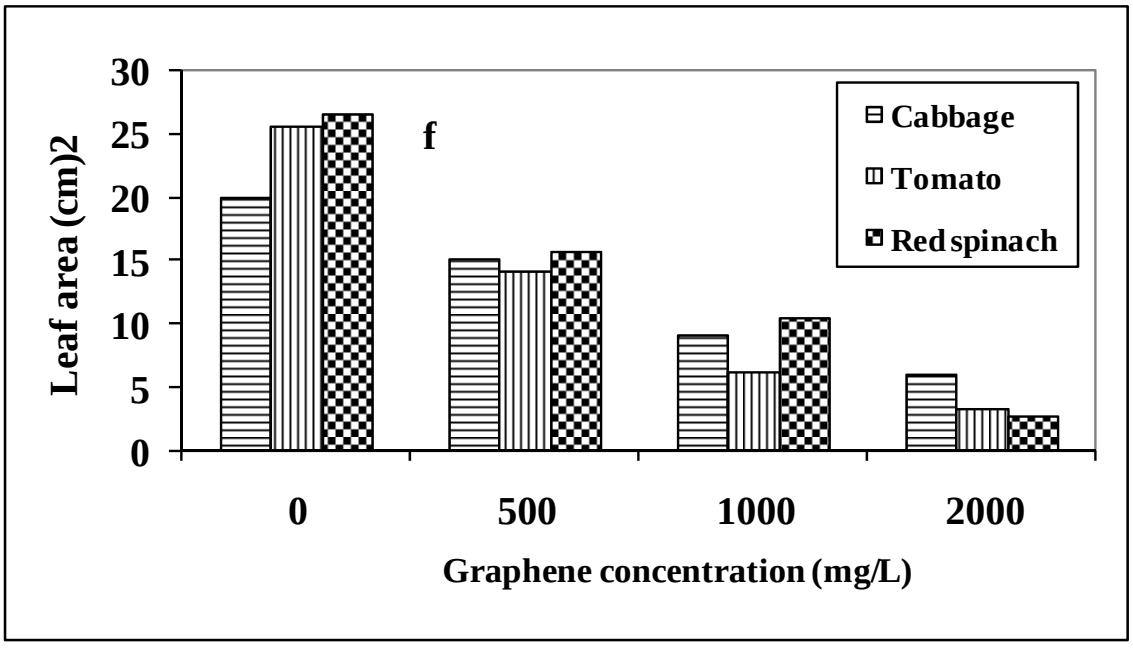
f
Leaf area (cm)2
30
25
20
15
10
5
0
Cabbage
Tomato
Red spinach
0
500
1000
2000
Graphene concentration (mg/L)

Fig. 5

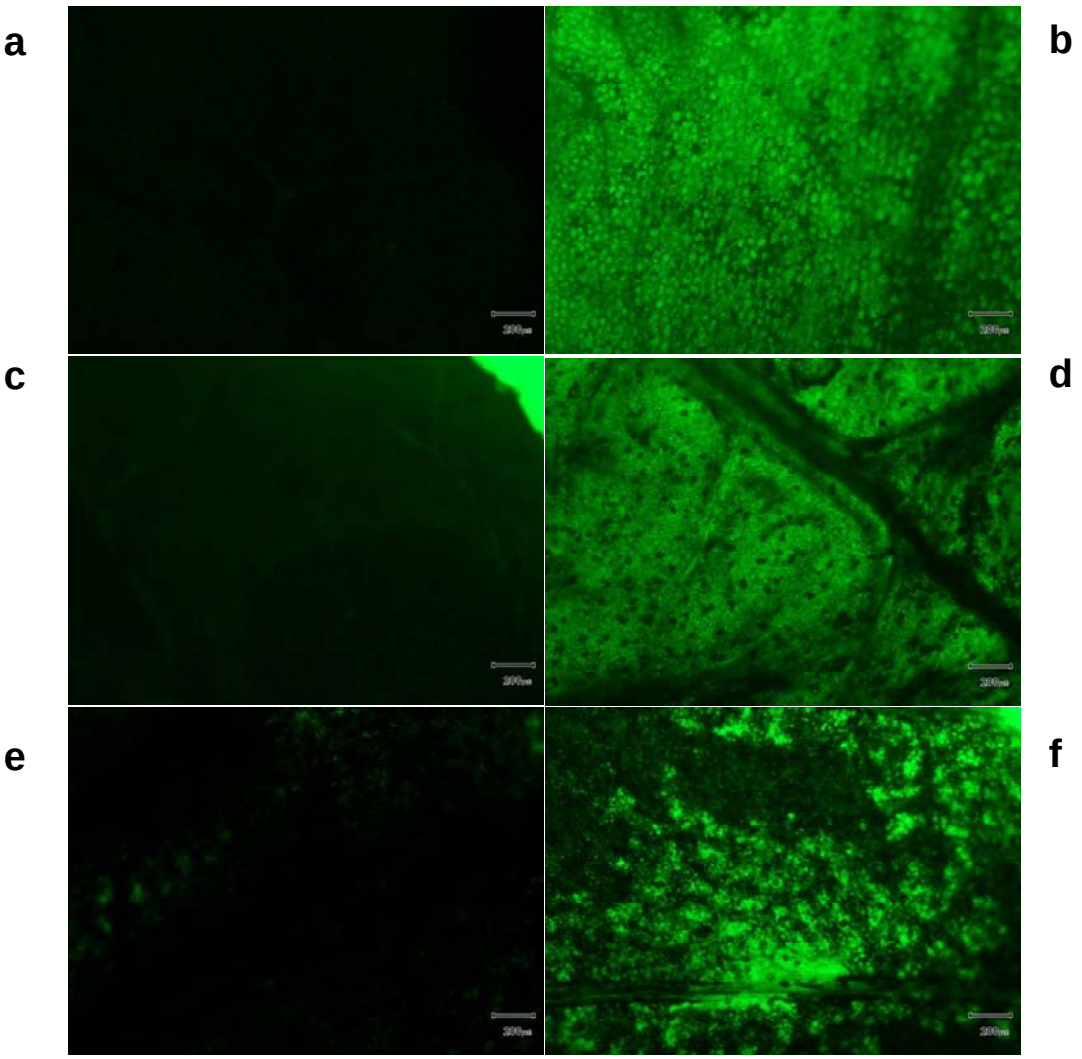
a
b
c
d
e
f

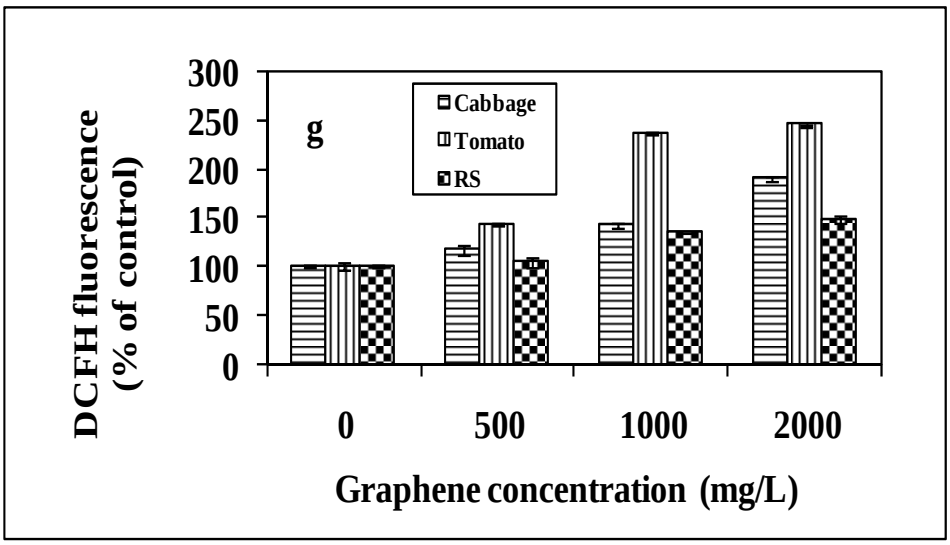
g
Cabbage
Tomato
RS
DCFH fluorescence (% of control)
300
250
200
150
100
50
0
0
500
1000
2000
Graphene concentration (mg/L)

Fig. 6

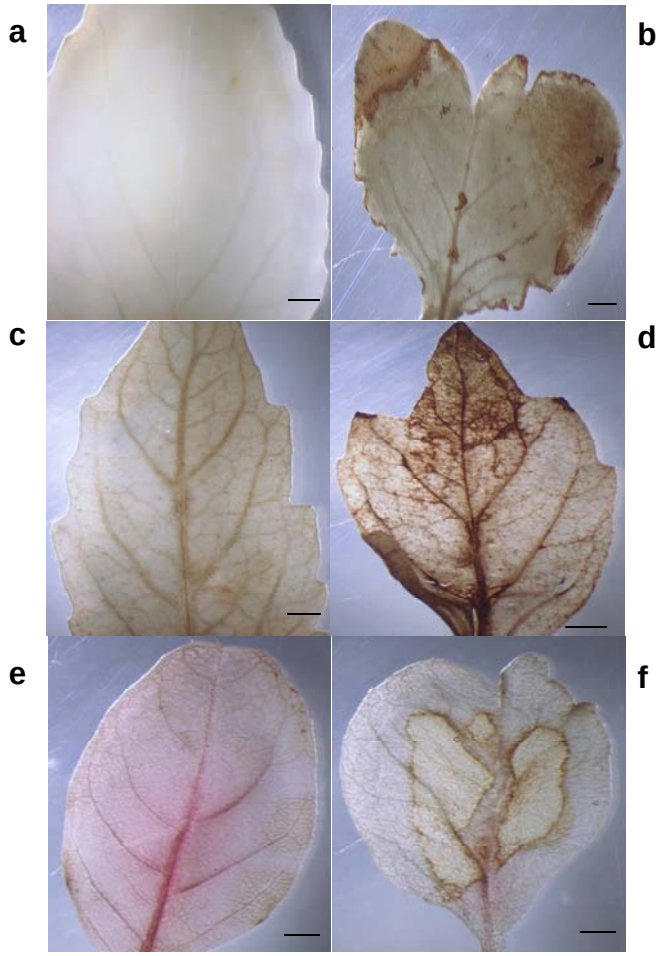
a
b
c
d
e
f

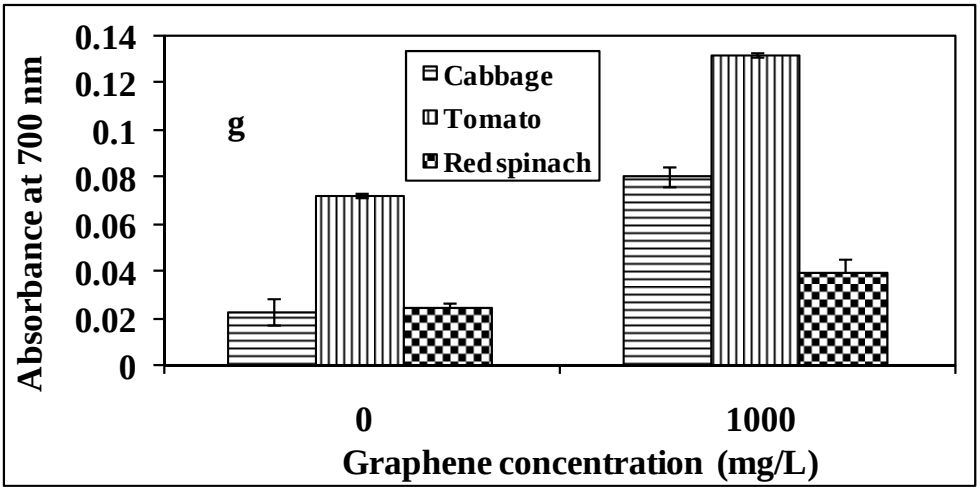
Absorbance at 700 nm
0.14
0.12
0.1
0.08
0.06
0.04
0.02
0
g
Cabbage
Tomato
Red spinach
0
1000
Graphene concentration (mg/L)

Fig. 7

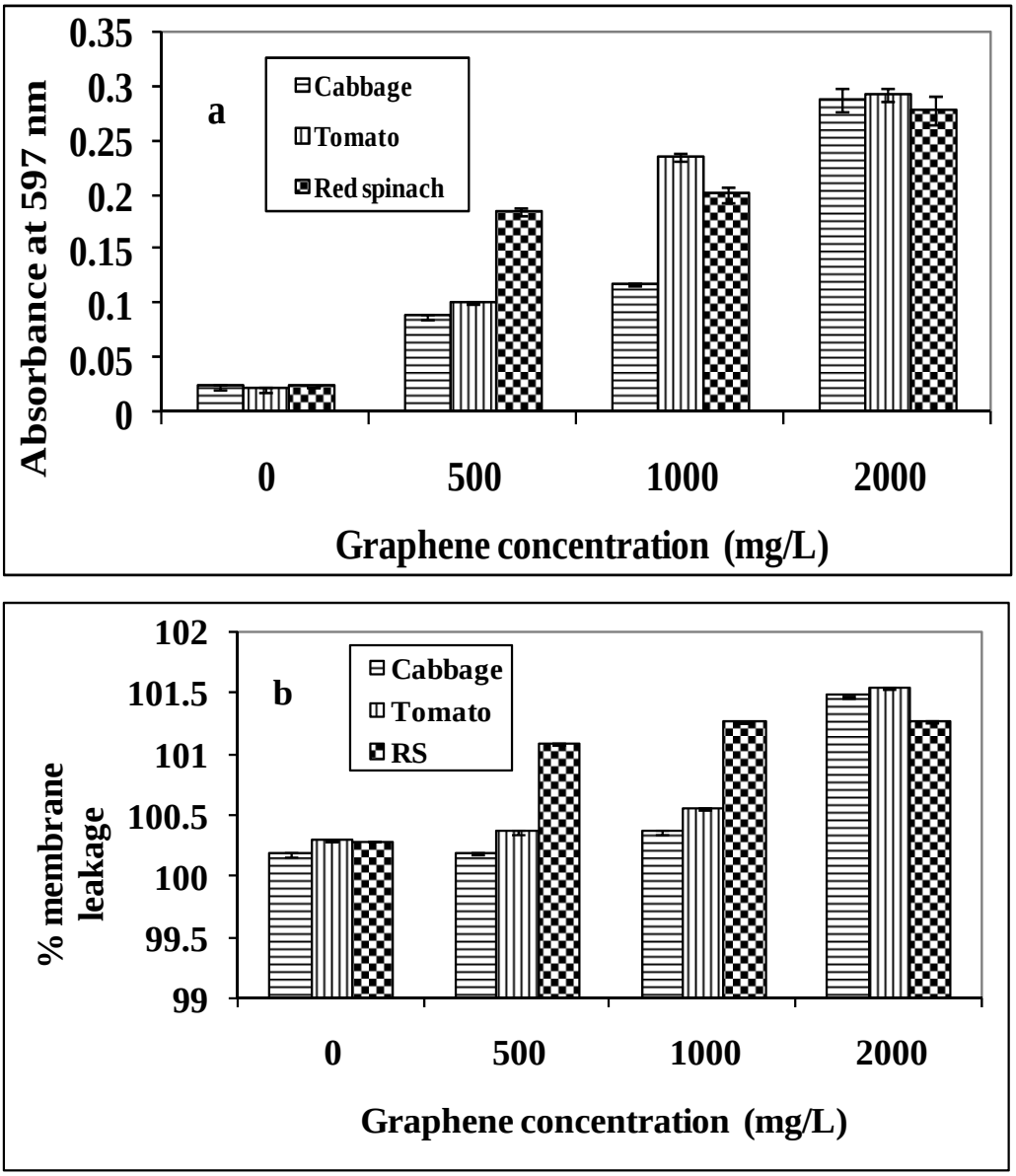
a
Cabbage
Tomato
Red spinach
Absorbance at 597 nm
0.35
0.3
0.25
0.2
0.15
0.1
0.05
0
0
500
1000
2000
Graphene concentration (mg/L)
b
Cabbage
Tomato
RS
% membrane leakage
102
101.5
101
100.5
100
99.5
99
0
500
1000
2000
Graphene concentration (mg/L)

Fig. 8

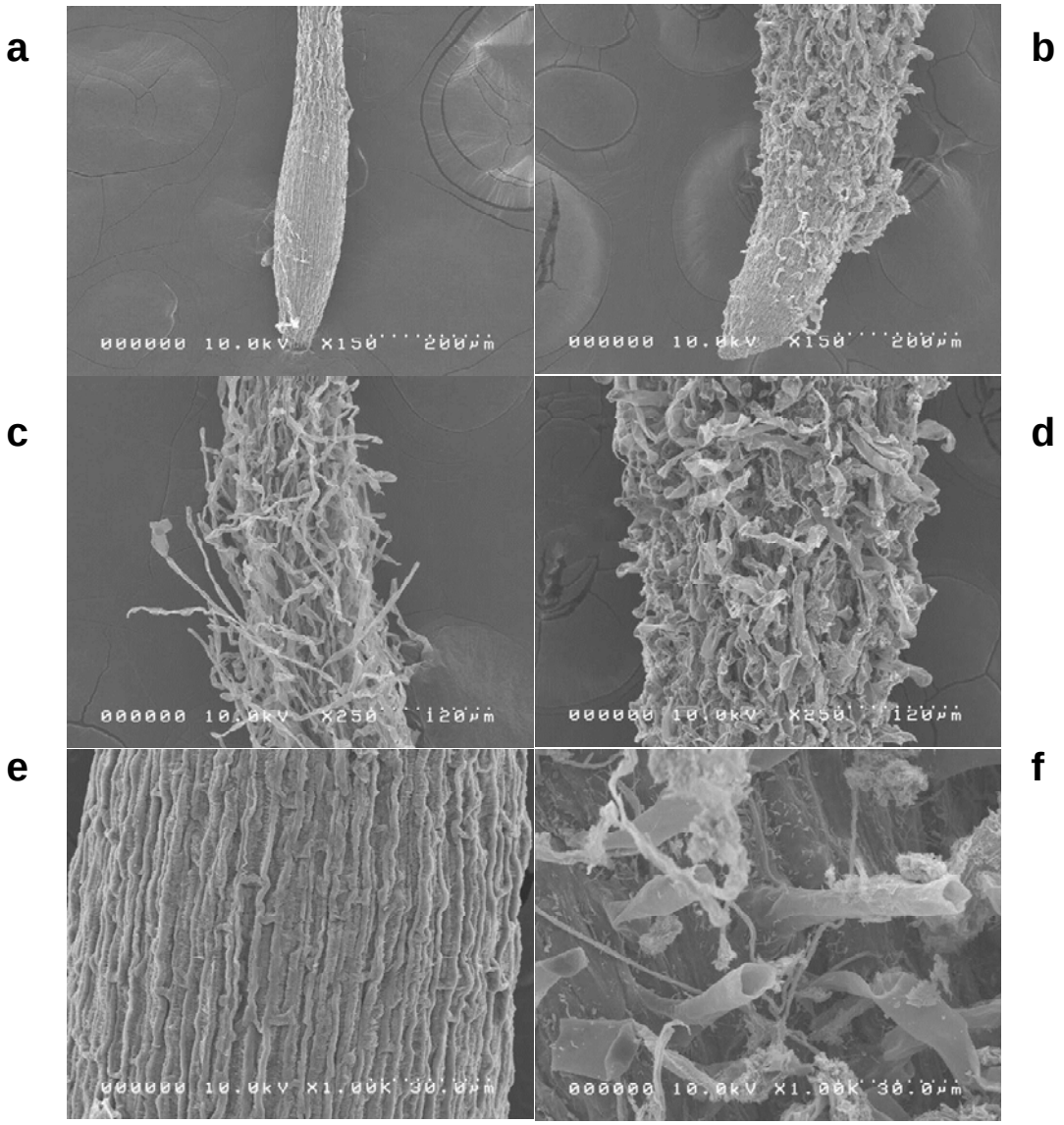
a
b
c
d
e
f
000000 10.0kV X150 200µm
000000 10.0kV X150 200µm
000000 10.0kV X250 120µm
000000 10.0kV X250 120µm
000000 10.0kV X1.00K 30.0µm
000000 10.0kV X1.00K 30.0µm

Fig. 9

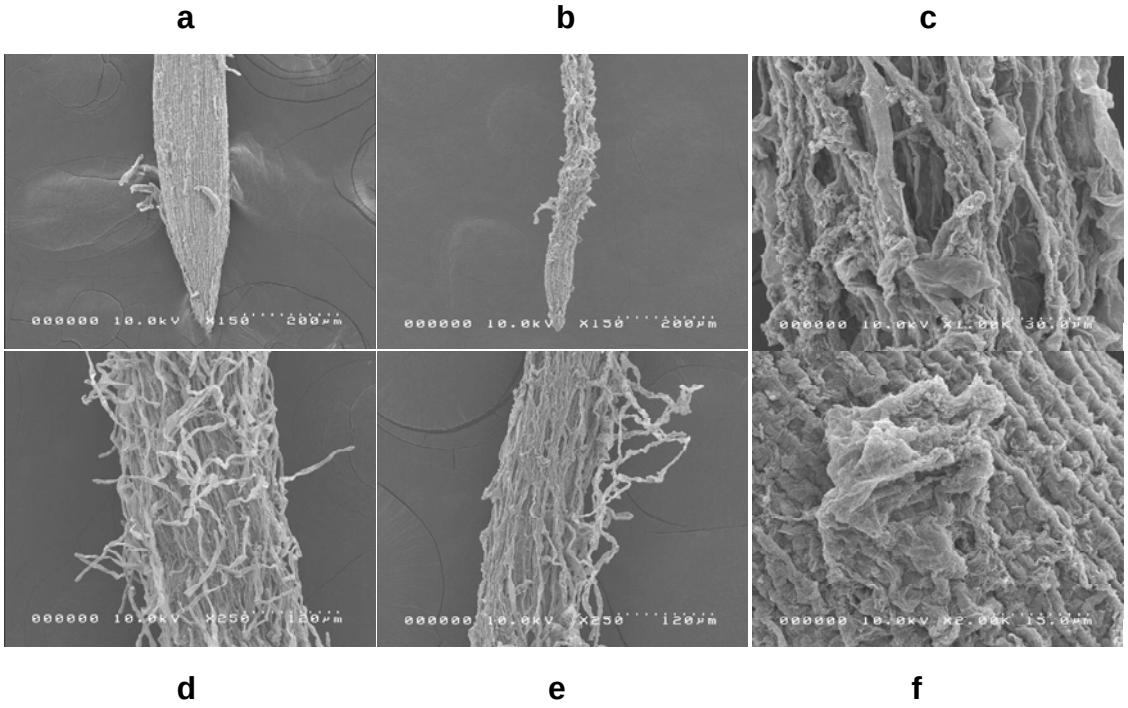

Fig. 10

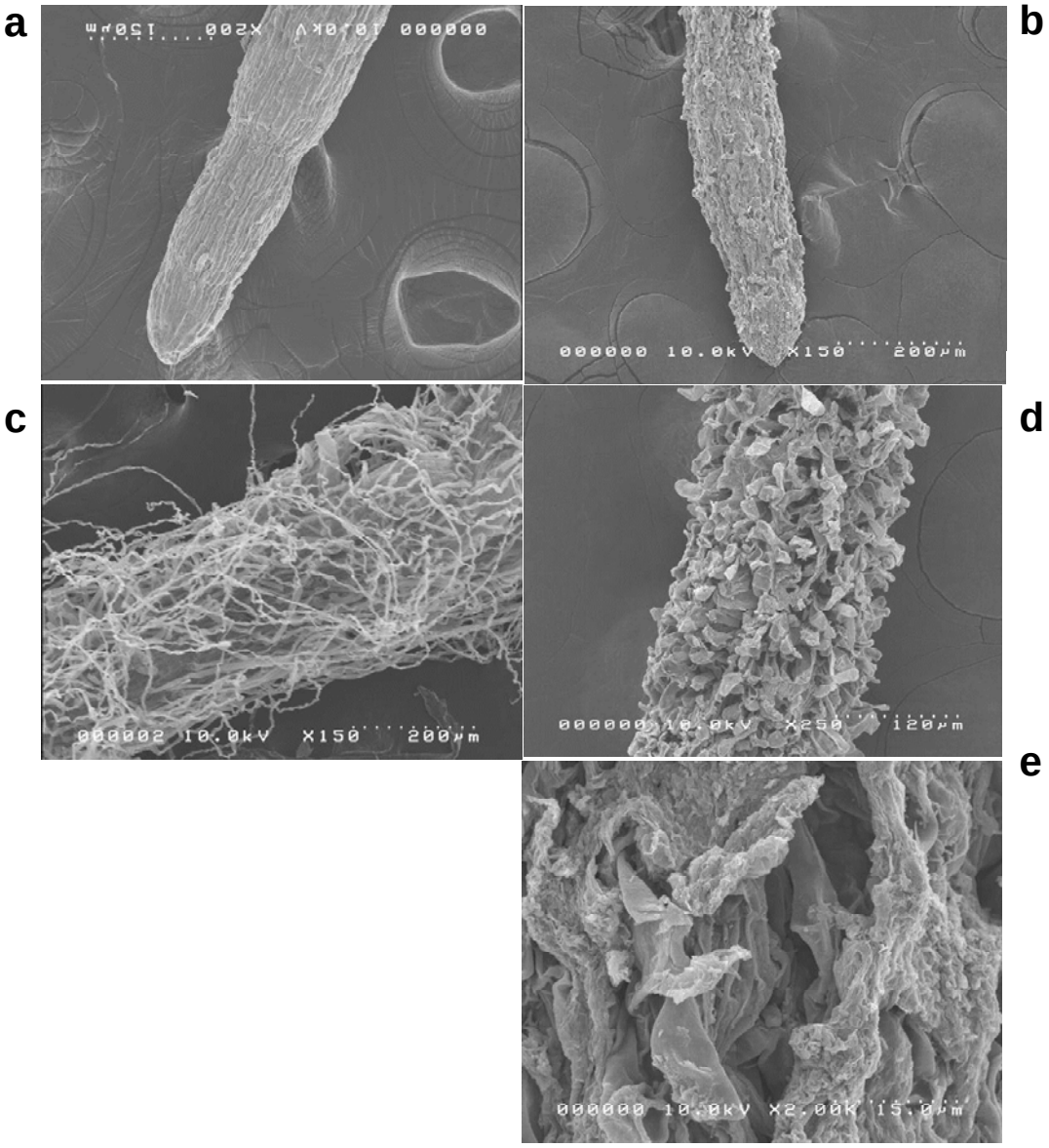
a
b
c
d
e
000000 10.0kV X150 200µm
000002 10.0kV X150 200µm
000000 10.0kV X250 120µm
000000 10.0kV X2.00k 15.0µm

Fig. 11